

Performance Analysis of Plain Journal Bearing Using CFD Model

M.M. Shahin, M.A. Chowdhury and M.H. Monir

Department of Mechanical Engineering, Dhaka University of Engineering and Technology
shahin.duet37@gmail.com

Abstract

Bearing stability depends on the slenderness ratio (L/D), lubricant film thickness, lubricant whirl frequency, lubricant oil temperature, lubricant pressure, attitude angle, stiffness coefficient, viscosity, lubricant density etc. Due to the friction force between shaft and bearing, bearing performance need to be determined according to different lubrication states and different geometry of the journal bearing, though it is difficult to find the performance using experiment. A new approach has been proposed in this study to determine the performance parameter using Ansys. The purpose of this study is to obtain an efficient slenderness ratio (L/D) by stiffness coefficient analysis on different coordinate of the journal bearing. It is a major concern to find out the viscosity and slenderness ratio (L/D) effects on bearing performance using CFD analysis. This is the first such type of study that the bearing performance has been conducted with 0.25 to 1.00 range of slenderness ratio and change of viscosity of lubricants by FLUENT 14.5. A Computational Fluid Dynamic (CFD) approach was applied which focused an optimized slenderness ratio range of 0.25 to 0.5 results lower elastic strain, deformation, and stress formation on the journal comparison to 1.00 L/D ratio.

Keywords: Journal bearing, Slenderness ratio, Viscosity, film thickness, SAE 5W-30

INTRODUCTION

Bearing geometry is a crucial parameter when selecting a proper bearing, and bearing geometry depends on the stiffness coefficient of hydrodynamic oil-lubricated plain journal bearings [1, 2]. A lubrication “wedge” forms in the hydrodynamic state, which lifts the journal, though journal also slightly shifts horizontally in the direction of rotation [3, 4]. The location of the journal is determined by the attitude angle and eccentricity ratio which are dependent on the direction and speed of rotation and the load [5-7]. The lubricant pressure also affects the eccentricity ratio in hydrostatic journal bearings. Friction force was observed from the arm of an applied load using a load cell. Many elements affect the friction coefficient, one of which is lubrication, here determined using SAE 5W-30 oil-lubricating gunmetal bearings since additional oil in the bearings considerably decreases the friction coefficient, especially at high velocities

and pressures [8, 9]. In addition, it has been observed that, the friction coefficient decreases using additional additives in lubricants [10], and the effect of loads, spindle speed, and oil types influence the friction coefficient [10, 11]. However, recently few studies have been investigated the optimal friction coefficient to improve the performance characteristics of a journal bearing [12-14]. Previous studies have determined different friction coefficient ranges using various lubricants according to different working conditions. Which is indicated higher friction coefficient and is not more applicable in practical application as well in rotating or reciprocating motion. Previous researcher did not study the bearing performance based on slenderness ratio or length-to-diameter ratio which has been presented in this study. During the change of shaft rotation, steady lubricant pressure is highly concerning issue to obtain a stabilizing

bearing stiffness coefficients (K) [15, 16] are introduced in this study which are not clear in previous literature. Bearings play the role like nature of the spring during applied load using stabilized bearing stiffness coefficients (K). Oil loses consistency as temperature builds, so insignificant varieties in ointment temperature was acquired which endorses the reasonableness of the oil in this study. The rudimentary prerequisite for hydrodynamic (oil wedge) is that oil of right thickness and adequate amount be available at all circumstances to surge the leeway spaces. The oil wedge shapes in a hydrodynamic bearing is an element of load (barrel weight), speed (RPM), and oil consistency (Z) at working temperature [17, 18]. Under fluid film conditions, an increase in viscosity or speed increases the oil film thickness and the coefficient of friction, while an increase in load decreases them. If the friction coefficient is reduced in increasing load (W) and speed (N) while viscosity remain constant, it can ensure the greater stability and better performance of bearings. The separate consideration of these effects presents an intricate picture that is simplified by combining viscosity Z, speed N, and load W, into a single dimensionless factor called the ZN/W factor [19]. Friction coefficient and film thickness of the bearing is proportional inversely and directly to the dimensionless factor ZN/W respectively [20]. Higher film thickness ensures the lower coefficient of friction that results remarkable higher lubricant pressure, minimal stress and deformation of the bearing was obtained at different slenderness ratio in this study. As the viscosity of oil, speed of the shaft and slenderness ratio are influence parameter to make reduced coefficient of friction which indicates the better performance (stress, pressure contours, deformation etc.) of the bearing [21], it is a major concern to and observe the change of

viscosity, speed and slenderness ratio effects on bearing performance using CFD analysis. This is the first such type of study that the bearing performance has been conducted using highly reduced friction coefficient which has been simulated using change of viscosity of lubricants and slenderness ratio by FLUENT 14.5. The Copper-base alloy (gun-metal) was considered in this study as the bearing material due to relatively cheap and easy to machine material, having good bearing properties and capable of withstanding somewhat higher loads than the other copper-base alloys. This alloy also has good resistance to corrosion in sea water. The effects of friction coefficient, viscosity, lubricant pressure and slenderness ratio were examined at different loads, speeds, and SAE 5W-30 oil-lubricated conditions. A new slenderness ratio ranges was proposed in this study which can be applied in practical application to get better performance of bearing.

Finally, in light of the outcomes, a range of slenderness ratio (L/D) also called slenderness ratio (λ) is proposed to obtain the optimal stiffness coefficients which indicate a higher bearing stability. There have been a few relevant study already conducted by the previous researchers, but there was no specific findings regarding the bearing stability on various slenderness ratio and lower stiffness was focused results lower stability of bearing. Other related bearing stability parameters using (Society of Automotive Engineers) SAE 5W-30 was obtained. Effective slenderness or length-to-diameter ratio (0.25L/D or 0.5L/D) was focused in this literature that provides remarkable journal bearing performance and durability under different working conditions. Due to optimal lubricant film thickness, the attitude angle was maintained within preferred ranges of 26 – 30 [22]. Lubricant film had an elasticity towards the radial direction of

the bearing due to minimum lubricant whirl in bearing shell which are novel findings in this study. Computational Fluid Dynamics (CFD) model was performed on

journal to find a safe value of slenderness ratio. The model of the current work has been validated and compared toward the work of Gertzos et al.[21, 23].

METHODOLOGY

Lubricant (SAE 5W-30) Properties

Table 1: A basic property of the tested SAE 5W-30SAE 5W-30 is a premium quality engine oil formulated from synthetic base oil with selected additives and has the highest performance level API service category SN. Some properties of the oil is shown in Table 1.

Appearance	Density at 15 °C (kg/m ³)	Kinematic viscosity at 40 °C (cSt)	Viscosity index	Flash point, °C	Pour point, °C	Total base no. mgKOH/g	Dynamic viscosity (Pa.s)
Clear	845	63	171	226	-33	7.62	0.053

Material properties

Gunmetal was selected as a journal bearing and SS304 was chosen as a shaft. The physical and mechanical properties and chemical composition of the journal bearing (gunmetal) are given in Table 2 and those of the journal shaft (SS304) are

given in Table 3. The bearings measured: length 100 mm, 50 mm, and 25 mm, inner diameter 100 mm and outer diameter 102.5 mm. The dimension of the journal shaft length was 350 mm with diameter 99.95 mm.

Table 2: Chemical composition and physical and mechanical properties of gunmetal journal bearings.

Chemical composition (%)					Mechanical properties		Physical properties		
Cu	Sn	Zn	Mn	Pb	TS (MPa)	BH No.	Sp. gravity	α (°C)	M.P. (°C)
85	5	5	1	4	221-310	65-74	8.719	18.72	1030

Table 3: Chemical composition and physical and mechanical properties of SS 304 journal shaft.

Chemical compositions (%)							Mechanical properties		Physical properties		
Mn	P	S	N	Si	Ni	Cr	TS (MPa)	BH No.	Specific gravity	α (°C)	M.P. (°C)
2	0.045	0.03	0.10	0.75	8	18	621	170	8.03	16.9×10^{-6}	1450

As radial clearance 0.25 mm, different load conditions (10 N, 20 N, and 30 N) and speeds (500, 750, and 1000 rpm) were used over 60 minutes operating time.

Isothermal and steady flow neglecting gravitational forces and with zero body forces were considered during CFD modeling. The journal is considered as a moving wall, in which there is only the tangential component of the rotational velocity. Negative pressures are set to zero in order to account for cavitation. The pressure at the sides of the bearing is set

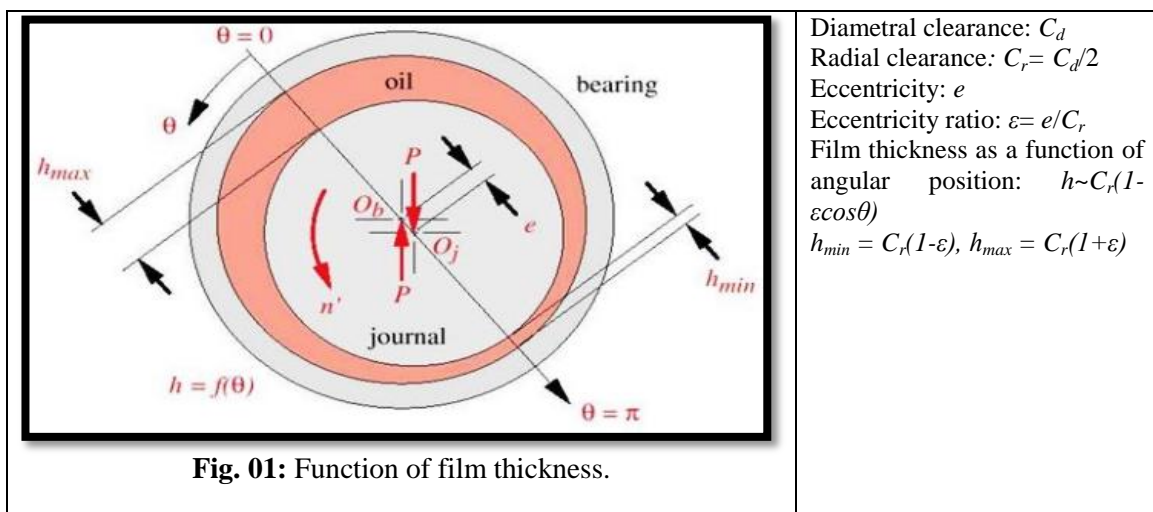
Analytical method

Assumptions and constraints

SAE 5W-30 flow conditions and model assumptions were considered in this study.

equal to zero, functioning as a free flow boundary. The model of the current work has been validated and compared toward the work of Gertzos et al.[21]. SAE 5W-30 lubricant flow in the journal periphery was considered laminar. The eccentricity ratio (ϵ) was considered as 0.2 ~ 0.7. Relative clearance $\psi = 0.001$, slenderness ratio $L/D = 0.25 - 1.00$, journal speed = 5.25 m/sec, load carrying capacity = 30 N, and 1 atm. operating pressure were considered the boundary conditions of the CFD model.

SAE 5W-30 lubricant film clearance was considered as an inlet but also alternating as an outlet of the bearing periphery. The outer periphery of the SAE 5W-30 film was modeled as a fixed boundary and the inner periphery was considered as a moving boundary with angular speed of the bearing in which slip between two boundaries was neglected. Some terminology of shaft and bearing under the load is shown in **Fig. 01**.



CFD Model

The CFD (FLUENT 14.5) was used to observe the effect of the other properties of the lubricant and bearing on the bearing performance. Total deformation, pressure contours, and equivalent stress were accurately observed using 16 divisions across the film thickness and 400 divisions in the circumferential direction. The applied load capacity W (30 N) of the journal bearing at diameter (100 mm) with different lengths (25 mm, 50 mm, and 100 mm) under different journal rotational speeds (500 rpm, 750 rpm, and 1000 rpm) were considered. Hexahedron grids were used as meshing. Different viscosities were considered in the model to compare other SAE based oil such as SAE-30, SAE10W-40 etc. SAE 5W-30 flow conditions and model assumptions were considered as an experimental study.

Isothermal and steady flow neglecting gravitational forces and with zero body forces were considered during CFD modeling. The journal is considered as a moving wall, in which there is only the tangential component of the rotational velocity. Negative pressures are set to zero in order to account for cavitation. The pressure at the sides of the bearing is set equal to zero, functioning as a free flow boundary. The eccentricity ratio (ϵ) was considered as 0.5. Relative clearance $\psi = 0.25$, slenderness ratio $L/D = 0.25, 0.5$ and 1.00, linear speed of the journal = 5.25 m/sec. Operating pressure were considered the boundary conditions of the CFD model. The outer periphery of the SAE 5W-30 film was modeled as a fixed boundary and the inner periphery was considered as a moving boundary with

angular speed of the bearing in which slip between two boundaries was neglected. **Fig. 02** indicates the boundary conditions.

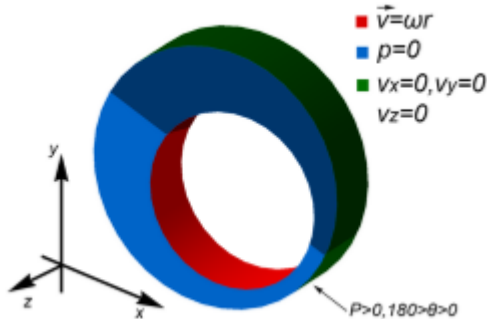


Fig.2: The boundary conditions of CFD model.

RESULT AND DISCUSSION

The pressure distribution was located along the midline of the plain journal bearing. The steady state condition was

assumed. The journal bearing fluid flow was considered laminar. The viscosity of lubricant was varied at only for L/D= 0.25 as a sample geometry to obtain the effects (pressure, stress, deformation etc.) of viscosity on bearings under different operating conditions. In this model (**Fig. 03**), a maximum pressure of $1.08E10^5$ Pa and a minimum pressure of $3.36E10^3$ at viscosity 0.05052 Pa.s and speed 500 rpm were observed. Maximum stress was obtained at viscosity 0.0637 Pa.s at 1000 rpm, as shown in **Fig. 04**. Maximum deformation was observed at viscosity 0.0637 Pa.s at 1000 rpm and minimum deformation was found at viscosity 0.0637 Pa.s at 500 rpm (**Fig. 05**). **Table 4** discusses the effect of change of viscosity of lubricant.

Table 4. Bearing performance measured using the CFD model at different viscosities. Due to change of viscosity using L/D = 0.25 as a sample slenderness ratio, different lubricant viscosities (0.05052 Pa.s, 0.052693 Pa.s and 0.0637 Pa.s) are presented.

Affected properties	0.05052 Pa.s			0.052693 Pa.s			0.0637 Pa.s		
	500 rpm	750 rpm	1000 rpm	500 rpm	750 rpm	1000 rpm	500 rpm	750 rpm	1000 rpm
Maximum pressure distribution/e+005 (Pa)	1.088	1.648	2.217	1.134	1.717	2.310	1.365	2.067	2.775
Maximum equivalent stress (MPa)	3.052	4.614	6.197	3.181	4.807	6.456	3.832	5.79	7.767
Maximum total deformation (mm)×10 ³	1.192	1.80	2.414	1.243	1.874	2.515	1.497	2.259	3.027

The operating lubricant (SAE 5W-30) viscosity and operating conditions is used in the model which affect the bearing. A maximum pressure was obtained at L/D ratio 1 and 1000rpm shown in **Fig. 06**, while **Fig.07** shows that the maximum equivalent stress was obtained at 1000 rpm and an L/D ratio of 1.00, while the minimum equivalent stress was found at

500 rpm and an L/D ratio of 0.25. It can be seen from **Fig. 08** that the maximum deformation was obtained at 1000 rpm and L/D ratio 1 and the minimum deformation was determined at 500 rpm and L/D ratio 0.25. **Table 5** shows the variations of performance due to change of slenderness ratio.

Table 5. Performance variation of bearings measured using the CFD model using different slenderness ratios. This table shows SAE 5W-30 lubricant viscosity 0.052693 Pa.s.

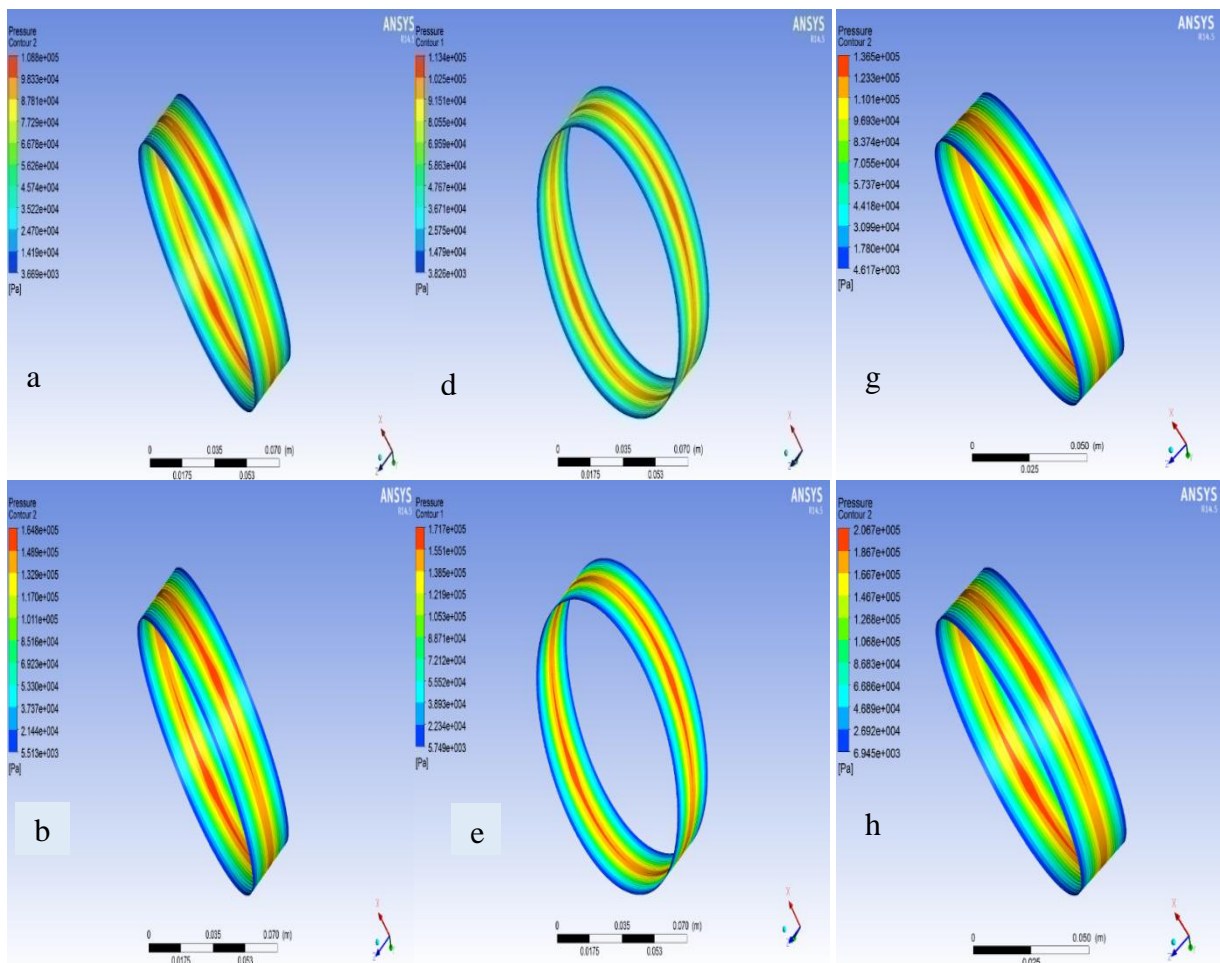
Affected properties	L/D= 0.25			L/D= 0.5			L/D=1		
	500 rpm	750 rpm	1000 rpm	500 rpm	750 rpm	1000 rpm	500 rpm	750 rpm	1000 rpm

Maximum pressure distribution/e+005 (Pa)	1.134	1.717	2.310	2.229	3.367	4.517	4.643	7.000	9.378
Maximum equivalent stress (MPa)	3.181	4.81	6.456	7.063	10.652	14.26	15.137	22.804	30.515
Maximum total deformation (mm)×10 ³	1.243	1.874	2.516	3.280	4.942	6.615	7.786	11.743	15.73

Comparison of pressure contour profiles for different viscosities

Fig. 03. (a - i) shows the pressure distributions for slenderness ratio L/D of 0.25 with changes in speed and lubricant viscosity 0.05052 Pa.s, 0.052693 Pa.s, and 0.0637 Pa.s. The maximum pressure contour was found by changing different parameters based on the experimental

conditions. A 1.33 –2.0 times change in journal bearing speed contributed increasing pressure up to 0.22% - 0.3% for 0.05052 Pa.s (**Fig. 03** a, b, and c), 0.052693 Pa.s (**Fig. 03** d, e, and f), and 0.0637 Pa.s (**Fig. 03** g, h, and i) at L/D=0.25. Film pressure was obtained up to 0.28% due to the change in viscosity up to 1.20 times at 500 rpm.



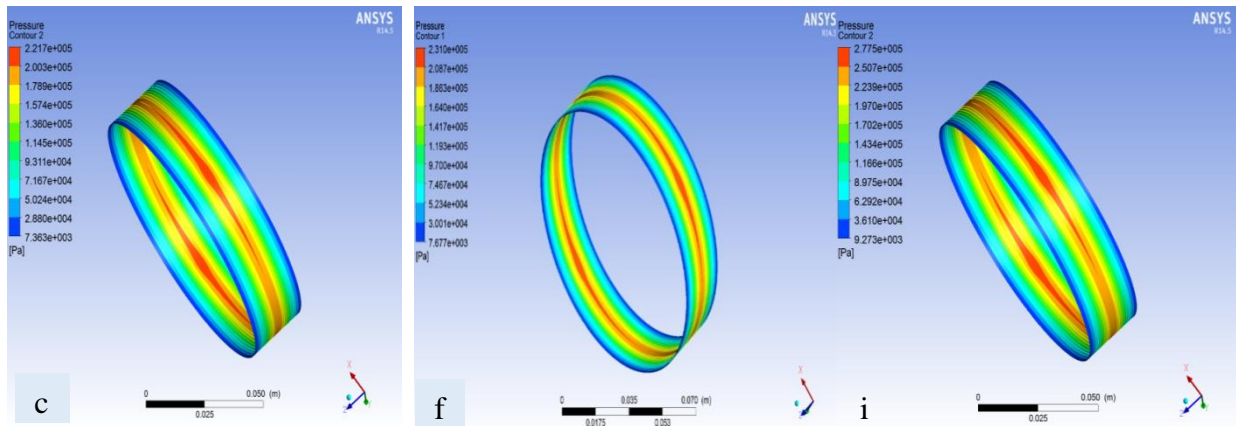
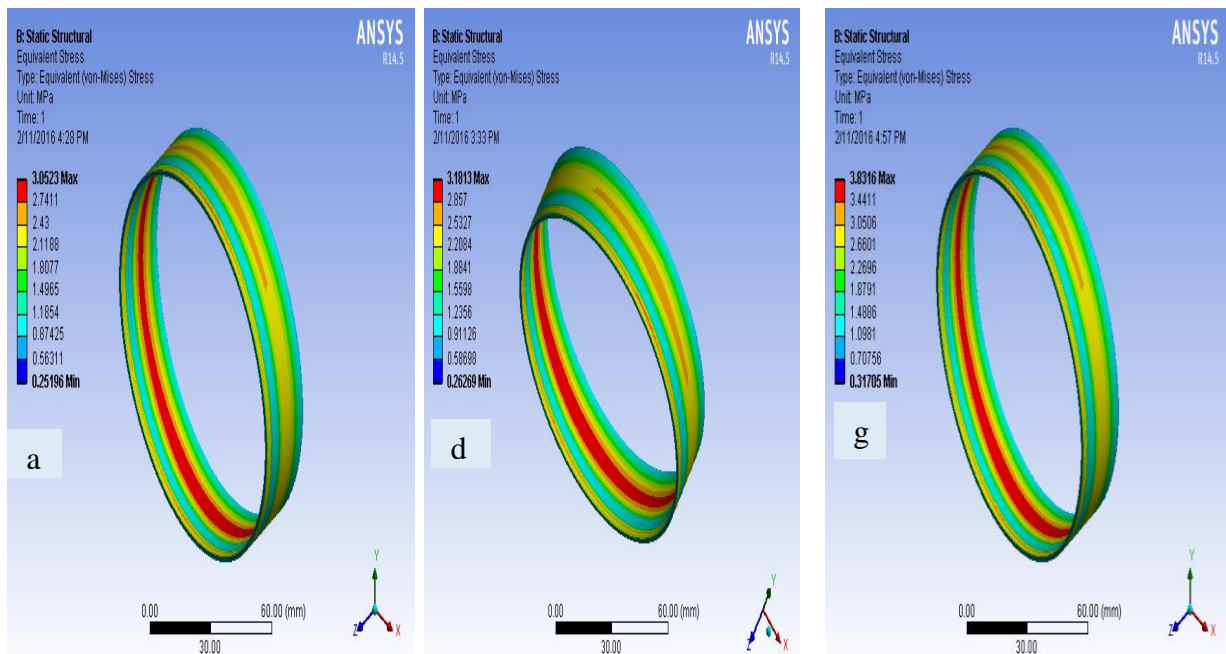


Fig.3. Comparison of pressure contour profiles at $L/D=0.25$ for: a) viscosity 0.05052 Pa.s ; 500 rpm , (b) viscosity 0.05052 Pa.s ; 750 rpm , (c) viscosity 0.05052 Pa.s ; 1000 rpm , (d) viscosity 0.052693 Pa.s ; 500 rpm , (e) viscosity 0.052693 Pa.s ; 750 rpm , (f) viscosity 0.052693 Pa.s ; 1000 rpm , (g) viscosity 0.0637 Pa.s ; 500 rpm , (h) viscosity 0.0637 Pa.s ; 750 rpm , (i) viscosity 0.0637 Pa.s ; 1000 rpm .

Change in equivalent stresses using different lubricant viscosities

Equivalent (von-Mises) stresses were obtained using ANSYS at $L/D=0.25$ for different oil-based lubricants as shown in **Fig. 04** (a - i). Using this information, an engineer can say his design will fail if the maximum Von-Mises stress value induced

in the material is greater than the strength of the material. This works well in most cases, especially when the material is ductile. **Fig. 04** shows 0.62%, 0.64%, and 0.77% changes in stress for 0.05052 Pa.s , 0.052693 Pa.s and 0.0637 Pa.s , respectively.



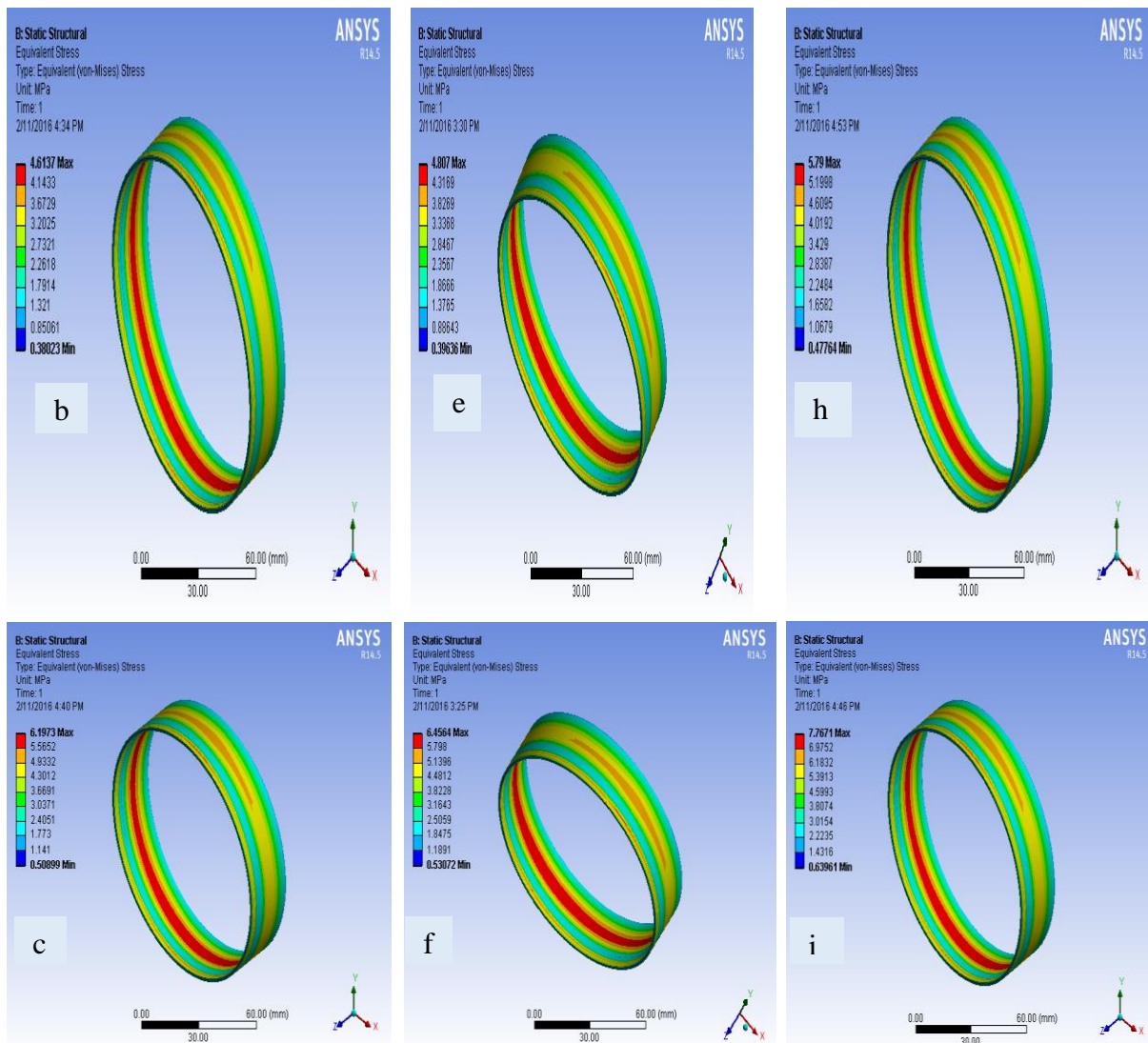


Fig. 4. Comparison of equivalent stress profiles at $L/D=0.25$ for: (a) viscosity 0.05052 Pa.s; 500 rpm, (b) viscosity 0.05052 Pa.s; 750 rpm, (c) viscosity 0.05052 Pa.s; 1000 rpm, (d) viscosity 0.052693 Pa.s; 500 rpm, (e) viscosity 0.052693 Pa.s; 750 rpm, (f) viscosity 0.052693 Pa.s; 1000 rpm, (g) viscosity 0.0637 Pa.s; 500 rpm, (h) viscosity 0.0637 Pa.s; 750 rpm, (i) viscosity 0.0637 Pa.s; 1000 rpm.

Change in total deformation using different lubricant viscosities

Bearings must be affected by the total deformation (in mm) found in this study. **Fig. 5** (a - i) introduces the maximum total deformation values. Lubricant viscosity 0.0637 Pa.s and journal speed 1000 rpm

produced a higher deformation of the bearing inner surface, as shown in **Fig. 5(i)**. The change in lubricant viscosity up to 1.25 times resulted in a large change in maximum deformation from 0.00030 to 0.00061.

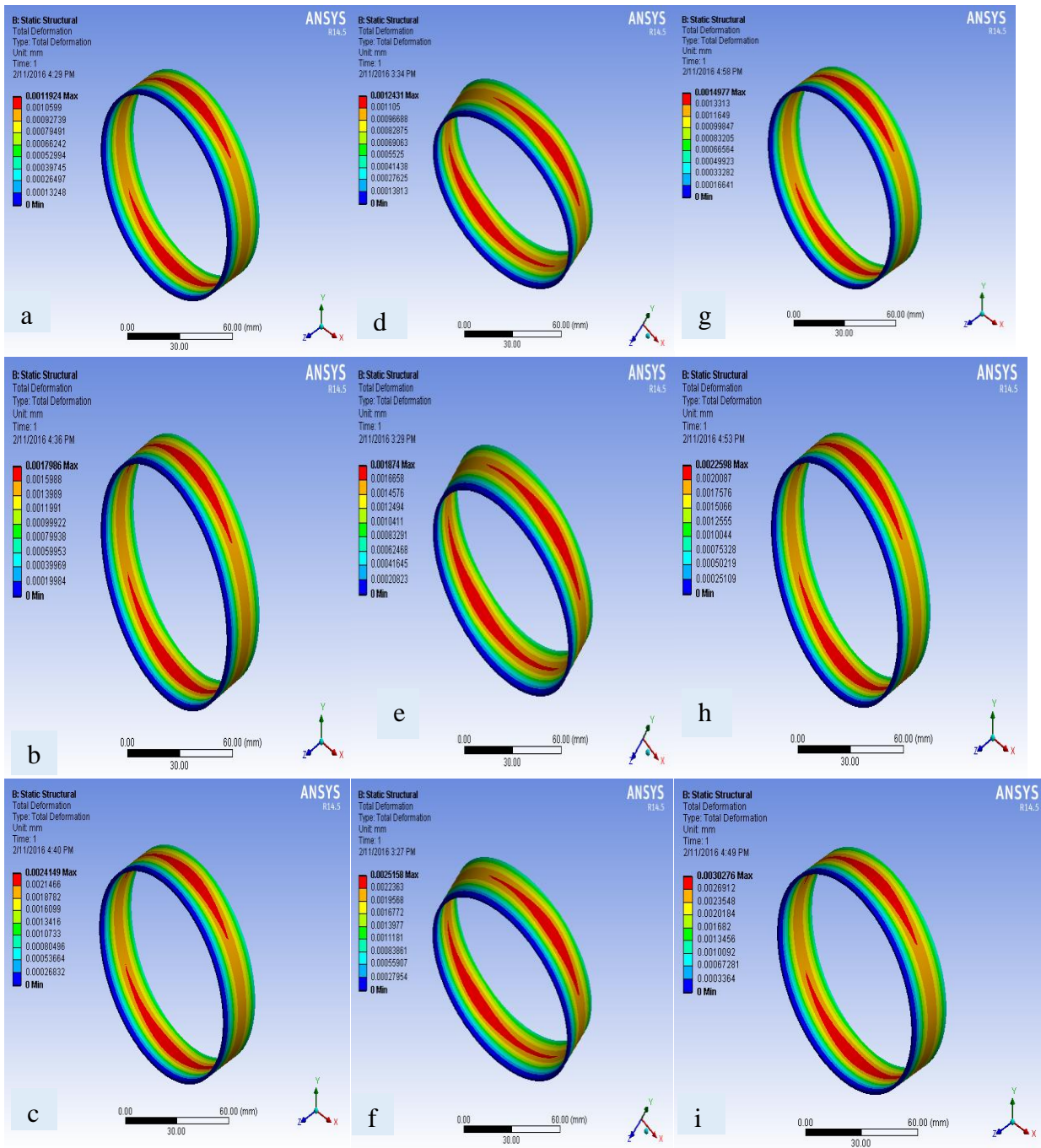


Fig. 5. Total deformation profile at $L/D= 0.25$ for: (a) viscosity 0.05052 Pa.s; 500 rpm, (b) viscosity 0.05052 Pa.s; 750 rpm, (c) viscosity 0.05052 Pa.s; 1000 rpm, (d) viscosity 0.052693 Pa.s; 500 rpm, (e) viscosity 0.052693 Pa.s; 750 rpm, (f) viscosity 0.052693 Pa.s; 1000 rpm, (g) viscosity 0.0637 Pa.s; 500 rpm, (h) viscosity 0.0637 Pa.s; 750 rpm, (i) viscosity 0.0637 Pa.s; 1000 rpm.

Pressure contour profiles for different slenderness ratios

Pressure distributions for different L/D ratios at various speeds between 500 to 1000 rpm for SAE 5W-30 oil lubricant (0.052693 Pa.s) were obtained as shown in

Fig. 06 (a - i). In this study, lubricant pressure increased by 0.23%, 0.45%, and 0.94% for slenderness ratios $L/D= 0.25$, $L/D= 0.5$ and $L/D= 1$, respectively. A lower film pressure indicates that the film thickness is discontinuous and results in a

reduction in the stability of the journal shaft on an eccentric center. The optimal film pressure was found at 0.5 slenderness

ratio at different rotational speeds, which can reduce perturbations in the journal bearing.

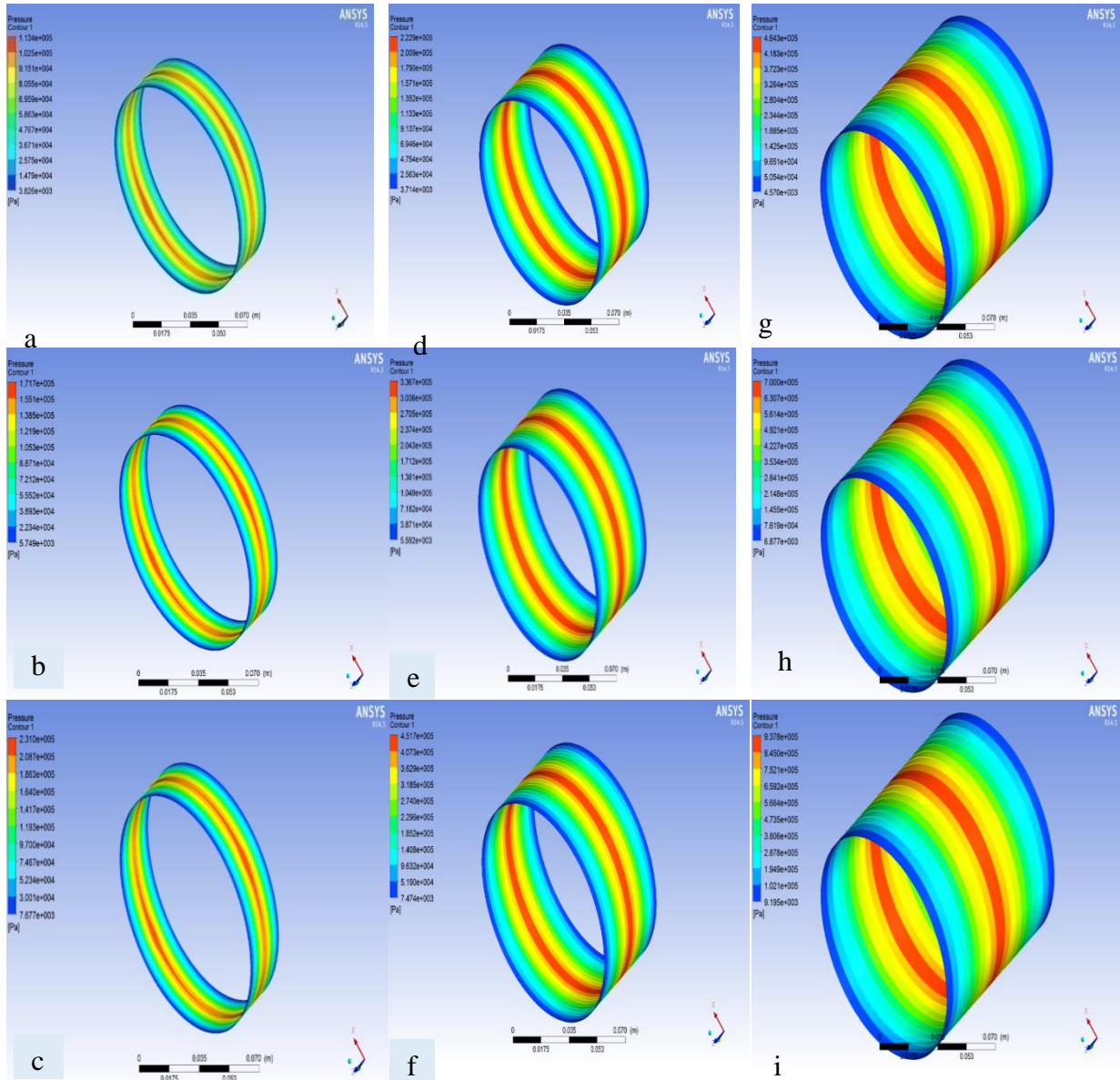


Fig.6. Comparison of pressure contour profiles of SAE 5W-30 with viscosity 0.052693 Pa.s at $L/D= 0.25$ for: (a) 500 rpm, (b) 750 rpm, and (c) 1000 rpm; at $L/D= 0.5$ for: (d) 500 rpm, (e) 750 rpm, and (f) 1000 rpm; at $L/D= 1$ for: (g) 500 rpm, (h) 750 rpm and (i) 1000 rpm.

Equivalent stress for different slenderness ratios

Bearing geometry has a large influence on bearing performance. Changes in slenderness ratios addresses changes in stress. **Fig. 07** (a - i) shows variations in equivalent von-Mises stress (MPa) using

0.052693 Pa.s (SAE 5W-30) with changes in slenderness ratio and journal speed. Equivalent stress was increased by 0.63%, 1.42%, and 3.05% for $L/D=0.25$, $L/D= 0.5$ and $L/D=1$ respectively. In this model, higher stress developed at maximum slenderness ratios at high speed.

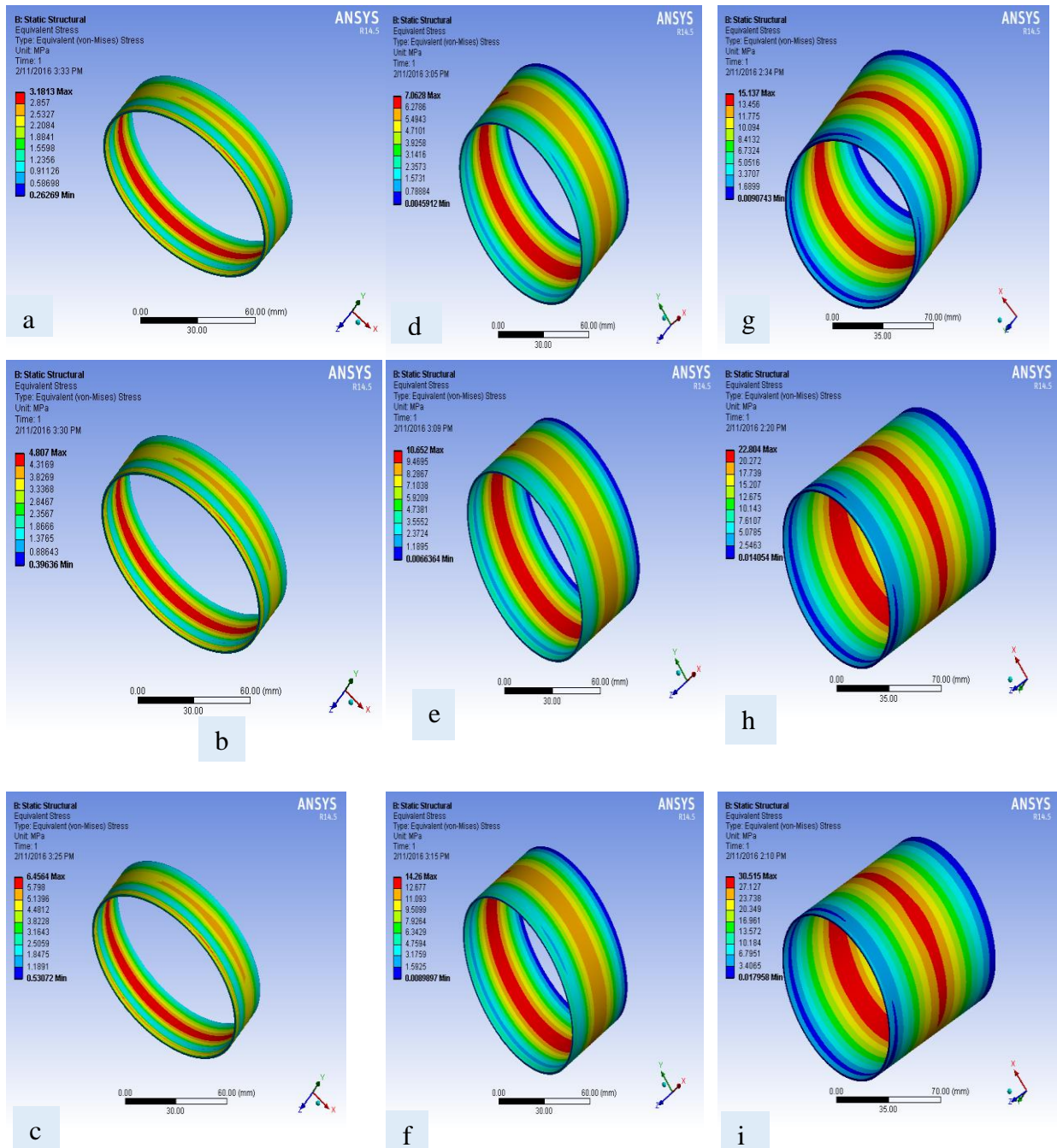


Fig. 07. Comparison of equivalent stress profiles of SAE 5W-30 viscosity 0.052693 Pa.s at $L/D=0.25$ for: (a) 500 rpm, (b) 750 rpm, and (c) 1000 rpm; at $L/D=0.5$ (d) 500 rpm, (e) 750 rpm, and (f) 1000 rpm; at $L/D=1$ (g) 500 rpm, (h) 750 rpm and (i) 1000 rpm.

Total deformation for different slenderness ratios

Bearings are highly affected by deformation. **Fig. 08** (a - i) shows the total deformation in mm with respect to different slenderness ratios with variations in speed. 0.052693 Pa.s (SAE 5W-30)

minimized bearing deformation from 500 rpm to 1000 rpm. A higher slenderness ratio of $L/D=1$ resulted in higher deformation of the bearing rather than lower L/D ratio, as shown in **Fig. 08**. (g, h, i). An L/d ratio of 0.25 – 0.5 may, therefore, may be more preferable for

reducing bearing deformation than higher slenderness ratios, especially $L/D > 1$.

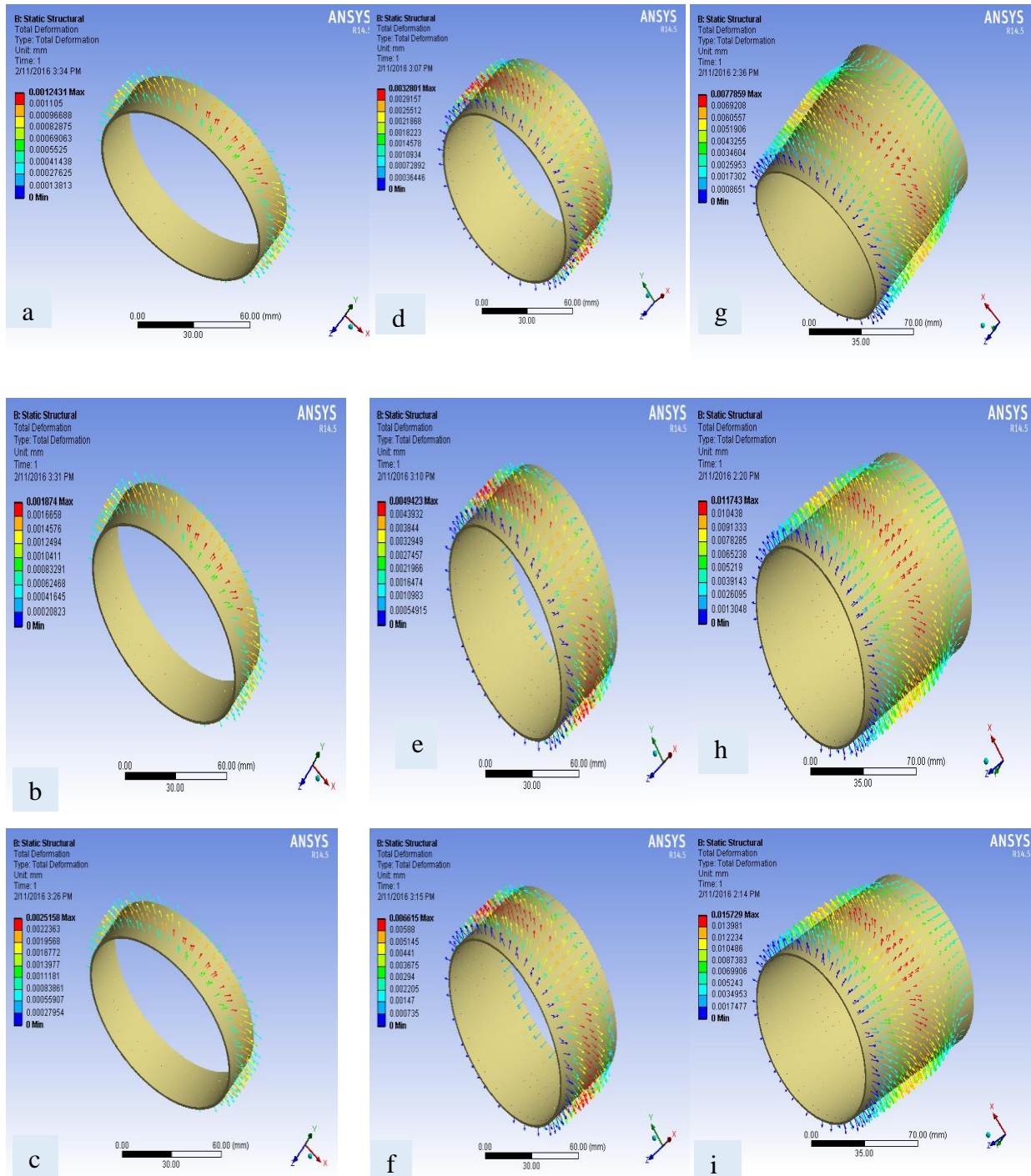


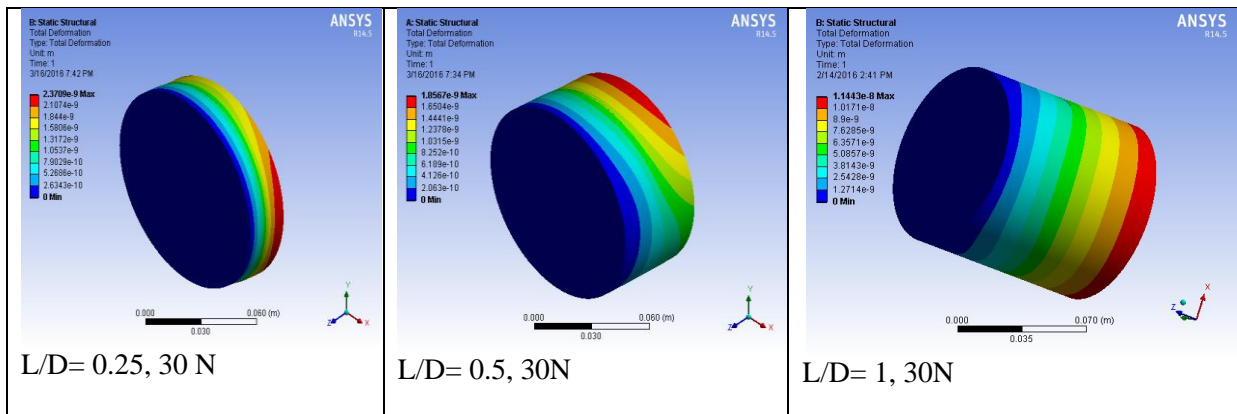
Fig. 8. Comparison of total deformation profiles of SAE 5W-30 viscosity 0.052693 Pa.s at $L/D=0.25$ for: (a) 500 rpm, (b) 750 rpm, and (c) 1000 rpm; at $L/D=0.5$ (d) 500 rpm, (e) 750 rpm, and (f) 1000 rpm; at $L/D=1$ (g) 500 rpm, (h) 750 rpm, and (i) 1000 rpm.

Comparison of deformation, elastic strain, and equivalent stress in shaft

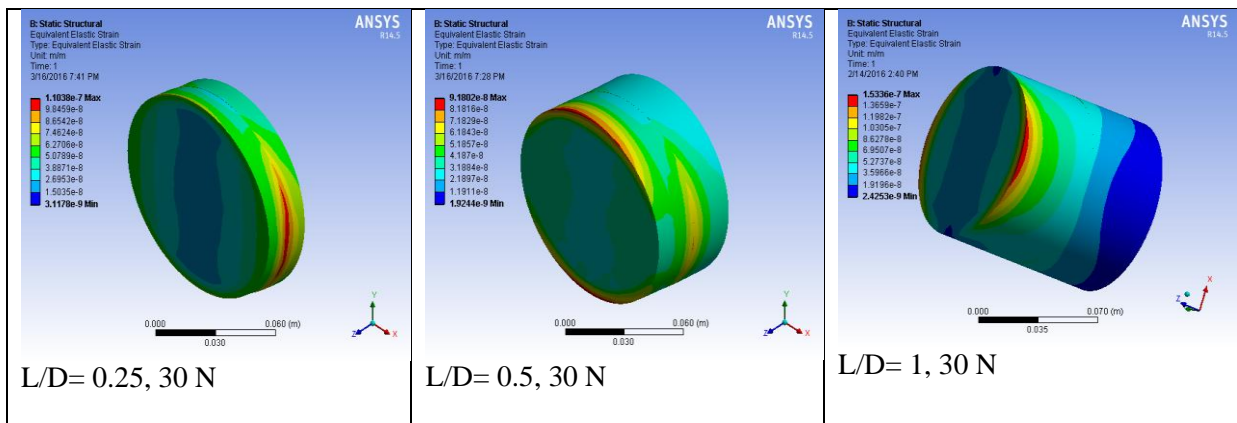
Fig. 09 (a), (b), and (c) show a comparison of deformation, elastic strain, and equivalent stress of the journal shaft using

the boundary conditions of 0.25, 0.50, and 1.00 slenderness ratio at 30 N load. Both lower (0.25) and higher (1.00) slenderness ratios produced greater deformation during CFD analysis due to improper piezo-viscous effects, while a 0.5 slenderness ratio generated a model with lower deformation. 0.25 to 0.50 slenderness ratios reduced 78.3% of the total deformation and 0.50 to 1.00 slenderness ratios increased 16.23% of the total deformation in CFD, as shown in **Fig. 09** (a). The distorted body returned to its original shape and size when the deforming force was removed (elastic strain). The effective Poisson's ratio will differ for each comparable elastic strain measurement [31, 41, 42]. **Fig. 09**(b) shows a comparison of equivalent elastic strains based on slenderness ratios at higher operating load capacity.

Intermediate operating slenderness ratio ($\epsilon = 0.5$) introduced lower elastic strain compared to 0.25 and 1.00 slenderness ratios in the CFD model. 0.5 L/D ratio at 30 N load capacity decreased the equivalent elastic strain by 83.16% and 60% compared to 0.25 and 1.00, respectively. **Fig. 09c** (i, ii and iii) differentiate the equivalent stresses of affected journal shafts with different L/D ratios at higher operating load capacity. Due to generating a proper SAE 5W-30 film thickness at 0.5 slenderness ratio, the equivalent stress was reduced by 80.00% and 58.00% compared to the 0.25 and 1.00 L/D ratios, respectively. In this study, CFD modeling successfully found a preferable dimension range of the journal bearing when operating conditions were varied by scale ratio.



a.



b.

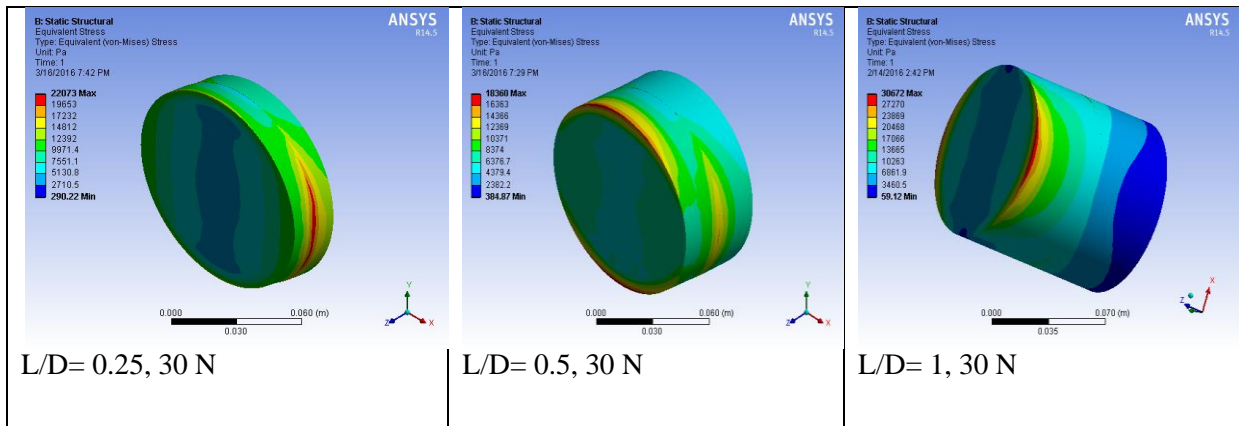


Fig. 09: Comparison of total deformation; (a), equivalent elastic strain; (b) and equivalent von-Mises stress; (c).

Comparison with different fluids

Stiffness coefficient (K) is the major factor which indicates stability of journal bearing. Stiffness coefficients (K), lubricant whirl frequency ratio (γ),

eccentricity ratio (ϵ) and attitude angles (θ) have been determined using SAE 5W-30 for a range of applied loads based on slenderness ratio (L/D) and Sommerfeld numbers is depicted in **Table 6**.

Table 6: Stability of journal bearing based on slenderness ratio (L/D) or slenderness ratio (λ) using SAE 5W-30 engine oil.

λ Or (L/D)	ϵ	W	$\theta_{Current}$	$\gamma_{Current}$	S	ϵ	Kxx \times E-08	Kyy \times E-08	Kxy \times E-08	Kyx \times E-08	Referen ces
0.25	0.3	10	36-38	0.314	0.25	-	-	-	-	4.5E3	[17, 43]
					0.30	-	7E3	4E3	7E2	-	
	0.4	20	33-34	0.280	0.4	-	-	-	-	-5.5E3	
					0.80	-	6.9E3	5E3	1.5E2	-	
	0.5	30	29-30	0.266	2.00	-	6.8E3	7E3	7E2	6.7E3	
0.50	0.3	10	39-40	0.289	0.25	0.47	-	-	-	[5, 14, 17]	

				[5, 14, 17]				
-7.8E3	-	-5.5E3	-4E3	-	-4	-	-2	
6E3	-	4.9E3	3E3	-	4	-	2	
2.2E3	-	2.4E3	2.5E3	-	0.1	-	0.11	
7E3	-	7.2E3	7.1E3	-	1.00	-	1.10	
0.40	0.33	0.27	0.15	-	-	-	-	
0.30	0.40	0.80	2.00	0.25	0.30	0.40	0.80	
0.272		0.261		0.365	0.361	0.356		
31-32		29-30		37-39	31-34	29-30		
20		30		10	20	30		
0.4		0.5		0.3	0.4	0.5		
1.00								

Attitude angle: θ , Slenderness ratio: L/D , Eccentricity ratio: ϵ , Sommerfeld No.: S , Applied load: W , Whirl frequency ratio: γ

CONCLUSIONS

CFD analyses were performed to investigate the influence of relative clearance (ψ), length-to-diameter ratio (L/D), slenderness ratio, diameter (D), applied load, and rotational speed (N) on stiffness coefficients. The viscous effect of SAE 5W-30 was taken into account in simulations. Pressure distributions and temperature variations at different bearing positions were observed to produce a lower viscous effect of SAE 5W-30. CFD model analyses revealed critical parameters and working conditions that are of practical use. The following conclusions can be drawn:

i. Bearing shows as like the nature of spring during applied load due to stiffness coefficient of the bearing.

Lubricant whirl approximately stable under higher applied load and speed.

- ii. The pressure of the oil film inside the journal bearing increased with increasing speed and load of the journal, especially increasing the slenderness ratio.
- iii. A slenderness ratio $L/D=0.5$ was optimal to generate the best position of film pressure from the x-x axis.
- iv. Using ANSYS, a 1.33 – 2.0 times change in journal bearing speed resulted in increasing pressure up to 0.22% - 0.3% for SAE 5W-30 (0.052693 Pa.s).
- v. Higher stresses was found for maximum slenderness ratios at high speed.

- vi. The CFD model suggested that an L/d ratio 0.25 – 0.5 was preferable for reducing bearing deformation compared to higher slenderness ratios, especially $L/D \geq 1$.

Acknowledgements

The authors would like to thank Dhaka University of Engineering & Technology for financial and technical support through Bangladesh National Scientific and Technical Documentation Centre (BANSDOC) and Bangladesh Atomic Energy Commission (BAEC).

REFERENCES

- Zhang, X., et al., *Determination of stiffness coefficients of hydrodynamic water-lubricated plain journal bearings*. Tribology International, 2015. **85**: p. 37-47.
- Hashimoto, H. and M. Ochiai, *Experimental study on the stabilization of small-bore journal bearings by controlling starved lubrication and bearing orientation angle*. Journal of Tribology, 2009. **131**(1): p. 011705.
- Litwin, W., *Experimental research on water lubricated three layer sliding bearing with lubrication grooves in the upper part of the bush and its comparison with a rubber bearing*. Tribology International, 2015. **82**: p. 153-161.
- Taylor, R.I., *Tribology and energy efficiency: From molecules to lubricated contacts to complete machines*. Faraday discussions, 2012. **156**(1): p. 361-382.
- Knauder, C., et al., *Analysis of the journal bearing friction losses in a heavy-duty diesel engine*. Lubricants, 2015. **3**(2): p. 142-154.
- Nikolakopoulos, P.G. and D.A. Bompos, *Experimental Measurements of Journal Bearing Friction Using Mineral, Synthetic, and Bio-Based Lubricants*. Lubricants, 2015. **3**(2): p. 155-163.
- Kasai, M., *Friction Reduction and Reliability Improvement of Plain Bearing Lubrication with Lubricating Automotive Engine Oil*. 2010, Université de Poitiers.
- Jang, J.Y. and M.M. Khonsari, *On the Characteristics of Misaligned Journal Bearings*. Lubricants, 2015. **3**(1): p. 27-53.
- Spencer, N.D., *Tribology*. Faraday discussions, 2012. **156**(1): p. 435-438.
- Durak, E., H. Koruca, and C. Kurbanoğlu. *Additional with additive decreases of friction at journal bearing*. in *Symposium of Mechanical Engineering*. 1999.
- Ahmad, M.A., S. Kasolang, and J.A. Ghani. *Effects of oil groove location on viscosity profile in hydrodynamic lubrication journal bearing*. in *Proceedings of Malaysian International Tribology Conference 2015*. 2015. Malaysian Tribology Society.
- Kasai, M., et al., *Influence of lubricants on plain bearing performance: Evaluation of bearing performance with polymer-containing oils*. Tribology International, 2012. **46**(1): p. 190-199.
- Jang, J.Y. and M.M. Khonsari, *On the Behavior of Misaligned Journal Bearings Based on Mass-Conservative Thermohydrodynamic Analysis*. Journal of Tribology, 2009. **132**(1): p. 011702-011702.
- Zhang, H., C. Zhu, and Q. Yang, *Characteristics of Micro Gas Journal Bearings Based on Effective Viscosity*. Journal of Tribology, 2009. **131**(4): p. 041707-041707.
- Nikolajsen, J.L., *The Effect of Variable Viscosity on the Stability of Plain Journal Bearings and Floating-Ring Journal Bearings*. Journal of Lubrication Technology, 1973. **95**(4): p. 447-456.
- Neacşu, I.A., et al., *Experimental Validation of the Simulated Steady-*

- State Behavior of Porous Journal Bearings*. Journal of Tribology, 2016. **138**(3): p. 031703-031703.
17. Offner, G., *Friction power loss simulation of internal combustion engines considering mixed lubricated radial slider, axial slider and piston to liner contacts*. Tribology Transactions, 2013. **56**(3): p. 503-515.
 18. Bompos, D. and P. Nikolakopoulos, *Journal Bearing Stiffness and Damping Coefficients Using Nanomagnetorheological Fluids and Stability Analysis*. Journal of Tribology, 2014. **136**(4): p. 041704.
 19. Hashimoto, H. and M. Ochiai, *Stabilization Method for Small-Bore Journal Bearings Utilizing Starved Lubrication*. Journal of Tribology, 2010. **132**(1): p. 011703.
 20. Matsumoto, K. and H. Hashimoto, *Study on Improvement of Stability of Noncircular Journal Bearing (Analysis of Stability in Case of Bearing Orientation Angle Change)*. Trans. Jpn. Soc. Mech. Eng., Ser. C, 2004. **70**(692): p. 1199-1206.
 21. Gertzog, K., P. Nikolakopoulos, and C. Papadopoulos, *CFD analysis of journal bearing hydrodynamic lubrication by Bingham lubricant*. Tribology International, 2008. **41**(12): p. 1190-1204.
 22. Guo, Z., T. Hirano, and R.G. Kirk, *Application of CFD analysis for rotating machinery—part I: hydrodynamic, hydrostatic bearings and squeeze film damper*. Journal of Engineering for Gas Turbines and Power, 2005. **127**(2): p. 445-451.
 23. Deligant, M., P. Podevin, and G. Descombes, *CFD model for turbocharger journal bearing performances*. Applied Thermal Engineering, 2011. **31**(5): p. 811-819.